Pmela and *Tyrp1b* Contribute to Melanophore Variation in Mexican Cavefish

Bethany A. Stahl, Connor R. Sears, Li Ma, Molly Perkins and Joshua B. Gross

Abstract Regressive evolution is a widespread phenomenon that affects every living organism, yet the mechanisms underlying trait loss remain largely unknown. Cave animals enable the study of degenerative disorders, owing to the frequent loss of eyes and pigmentation among lineages evolving in the subterranean habitat. Here, we utilize the blind Mexican cavefish, *Astyanax mexicanus*, to investigate regressive loss of pigmentation because "ancestral" surface-dwelling morphs allow direct comparisons with cave-dwelling forms. Two genes (*Oca2*-albinism and *Mc1r-brown*) have been linked to specific pigmentation alterations in several cavefish populations. Pigment cell (melanophore) number is a complex trait governed by multiple genes, and variation in this trait may contribute to pigmentation diversity in *Astyanax*. To uncover genes associated with this trait, we assembled a high-resolution linkage map and used automated phenotypic scoring to quantify melanophore number variation across seven body regions in a surface × Pachón cave F_2 pedigree. QTL mapping yielded several markers strongly associated with melanophore number variation in the dorsal mid-lateral stripe area and superior head region, which anchor to regions of the *Astyanax* genome and the zebrafish genome. Within these syntenic regions, we identified two candidate genes, *Tyrp1b* and *Pmela,* with known roles in pigmentation based on gene ontology annotation. Mutant forms of these candidate genes in other organisms cause global and regional pigmentation variation, respectively. In *Astyanax*, these genes harbor coding sequence mutations and demonstrate differential expression in Pachón cavefish compared to surface morphs. In sum, this work identifies genes involved with complex aspects of *Astyanax* pigmentation and provides insight into genetic mechanisms governing regressive phenotypic change.

B. A. Stahl · C. R. Sears · L. Ma · M. Perkins · J. B. Gross (✉)
Department of Biological Sciences, University of Cincinnati, Cincinnati, OH 45221, USA
e-mail: grossja@ucmail.uc.edu

Present Address
B. A. Stahl
Jupiter Life Science Initiative, Florida Atlantic University, Jupiter, FL 33458, USA

3

1 Introduction

Pigmentation varies dramatically across the animal kingdom—from crypsis to colorful ornamental displays—suggesting that coloration serves dynamic and adaptive functions. In many animals, these roles vary from mate choice selection (Protas and Patel 2008), defense from predation (Linnen et al. 2009), UV protection, structural support, and thermoregulation (Hubbard et al. 2010). Pigmentation traits have also served as a powerful approach for linking specific genes to phenotypic characters (Hoekstra 2006).

In this study, we investigated the naturally occurring pigmentation loss in the blind cavefish *Astyanax mexicanus* (Jeffery 2001; Borowsky 2008). This species harbors two distinct morphotypes: a pigmented surface-dwelling form that populates the rivers of NE Mexico, and several depigmented (or albino) cave-dwelling morphs that reside in the subterranean environment. This species demonstrates recurrent loss since *Astyanax* cave morphs have repeatedly colonized the cave, providing natural biological "replicates" (Gross 2012a).

The gene underlying the absence of melanin (albinism) was identified and confirmed by CRISPR mutagenesis in surface fish, as *Oca2* in two independent cavefish lineages (Protas et al. 2005; Gross and Wilkens 2013; Ma et al. 2015; Klaassen et al. 2018). A second pigmentation phenotype, *brown,* is associated with the gene *Mc1r* in three cavefish populations (Gross et al. 2009). Although these studies have discovered the genetic basis for monogenic components of pigmentation loss, the genes contributing to complex pigmentation loss in cavefish have not been identified. A prior mapping study in *Astyanax mexicanus* did confirm that melanophore (pigment cell) numerical variation is indeed complex and linked to 18 QTL associated with pigment cell number, yet the identity of the genes underlying this trait still remains unknown (Protas et al. 2007).

The previous characterization of melanogenesis in other animals shows that melanophores are derived from a set of migratory cells that give rise to numerous cell types including cranial cartilage and bone, peripheral neurons, fat cells, and pigment-producing melanophores (Erickson and Perris 1993; Huang and Saint-Jeannet 2004). Due to the diversity of neural crest cell derivatives, it would be less likely to acquire mutations within genes of the neural crest pathway due to potentially lethal consequences (Jeffery 2009). Labeling experiments revealed normal neural crest migration during cavefish development (McCauley et al. 2004), and quantification of cell apoptosis after neural crest-derived precursor migration showed comparable numbers in both cavefish and surface (Jeffery 2006). These combined results suggest that evolutionary changes leading to pigment cell regression in cave morphs may be mediated by alterations late in melanogenesis (Jeffery 2009).

To identify pigmentation-related genes, we employed a second-generation linkage map (Carlson et al. 2015) inclusive of >3,000 genomic markers to perform high-resolution mapping of melanophore number diversity in a large cave × surface F_2 pedigree (Fig. 1a–e). A quantitative trait locus (QTL) mapping study yielded numerous significant associations linked with 20 different regions of our linkage
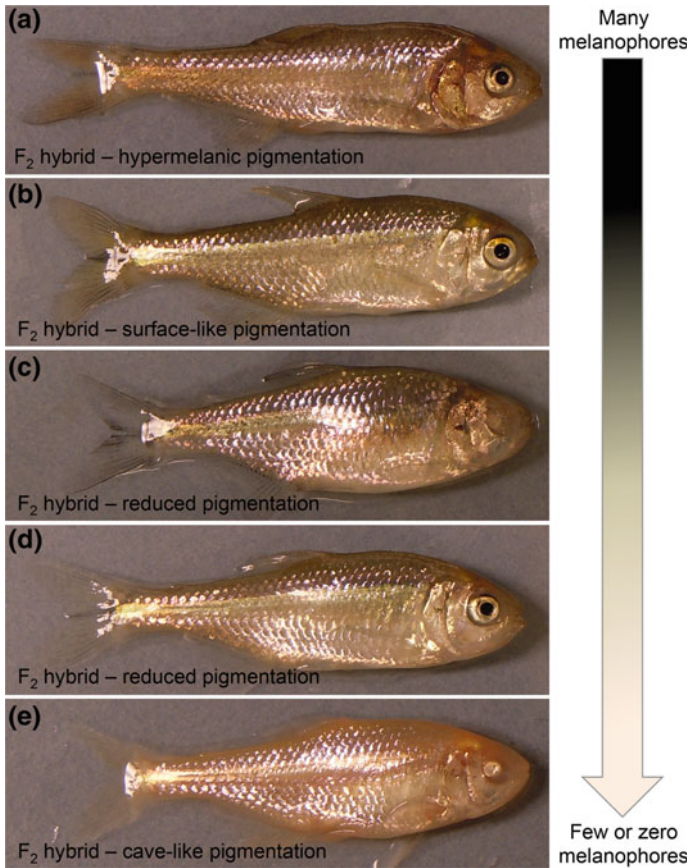
Fig. 1 Surface × Pachón cave F₂ sibling hybrids display a vast array of coloration. Hybrid offspring from a surface × Pachón cave cross reveal a varying degree of melanic-based pigmentation. The "dark" versus "light" appearance is associated with the number of melanophores (pigment cells) that an individual harbors. We observed levels of pigmentation that are darker (**a**) than normal surface fish (**b**). Some hybrid individuals showed dramatic reductions in pigmentation (**c**, **d**), while albino individuals (which still retain melanophores) produce no melanin, rendering melanophores invisible (**e**)

map. We then leveraged available genomics resources (McGaugh et al. 2014) to nominate candidate genes. Comparative genomics identified the critical syntenic region for each QTL in the *Astyanax* cavefish draft genome alongside conserved intervals in the distantly related zebrafish genome. We nominated candidate genes by screening the genes within these syntenic regions for gene ontology (GO) terms related to pigmentation. These analyses yielded two genes, *Tyrp1b* and *Pmela,* with well-characterized roles in melanin-based pigmentation in other animals. We further characterized the coding sequence and expression of candidate genes. Through these studies, we propose *Tyrp1b* and *Pmela* as genes that likely contribute to complex

pigmentation in *Astyanax* cavefish. Identification of additional pigmentation genes provides a clearer picture of the mechanisms contributing to regressive evolution in *Astyanax* and informs our understanding of the broader principles governing trait loss in the natural world.

2   Materials and Methods

2.1   Melanophore Scoring

To quantify melanophore number, we analyzed numerous regions of the body where pigment cell number varied within our F_2 pedigree. These included seven regions: near the anal fin (MelAnalfinSquare), below the mid-lateral stripe (MelUnderStripe), dorsal square (MelDorsalSquare), area above the stripe (MelAboveStripe), above the eye (MelHeadSquare), full head (MelHead), and neighboring the anal fin (MelAnalfinTriangle). Regions were selected based on a consistent set of landmarks for reproducibility and were similar to the areas previously assayed (Protas et al. 2007). For automated counts, we employed ImageJ (v.1.6; National Institutes of Health, Bethesda, MD) by inverting the color in a selected area and then counting the lighter objects (e.g., pigment cells, now white) with a preset "noise tolerance." The noise tolerance was set so only markings (melanophores in this case) above the preset light pixel intensity were counted. Each image was reviewed and any melanophores "missed" in the automatic quantification were manually added. When appropriate, we transformed the melanophore counts to $\log^{10}$ values to generate a normal distribution for association studies.

2.2   Quantitative Trait Locus (QTL) Association Mapping

All QTL analyses were performed using a previously published linkage map (Carlson et al. 2015). We employed the software program R/qtl (v.1.30; Broman et al. 2003) for all association analyses. We analyzed each trait using four mapping methods: marker regression (MR; Kearsey and Hyne 1994), expectation maximization (EM; Xu and Hu 2010), Haley-Knott (HK; Haley and Knott 1992), and nonparametric (NP; Kruglyak and Lander 1995) as described in Gross et al. (2014). Significant linkages were set at a LOD score threshold of ≥ 4.0—as used in other QTL studies (Protas et al. 2007; Gross et al. 2009). To confirm associations, permutation tests involving 1000 iterations were performed to identify statistically significant QTL ($P < 0.05$). Effect plots for associations were generated using the closest linked genetic marker. QTL regions were then anchored (~6–8 cM on each side of the top marker) using the NCBI BLAST Toolkit (v.2.28+) to the *Astyanax* genome (Ensembl build v.75; McGaugh et al. 2014). We also determined the syntenic interval in the zebrafish

genome, with previously demonstrated synteny with *Astyanax* (Gross et al. 2008; O'Quin et al. 2013; Carlson et al. 2015). Visual representations of synteny between our linkage map and the genomes were created with Circos (v.0.64; Krzywinski et al. 2009; Fig. 3a, d).

2.3 *Gene Ontology (GO) Term Analysis*

To nominate prospective candidate genes, we interrogated all genes within the syntenic interval in the *Astyanax* draft genome for gene ontology (GO) terms. From these analyses, we collected the GO terms for all genes located in the *Astyanax* syntenic interval using BioMart (v.0.8; Kasprzyk 2011). This approach yielded hundreds of GO terms for each significant QTL. We then narrowed our search to terms with potential involvement in pigmentation, such as "pigment", "pigmentation", "melanin", "eumelanin", "phaeomelanin", "melanophore", "melanocyte", "melanosome", "xanthophore", "iridophore", "chromatophore", and "carotene". This approach enabled the selection of genes based on annotation information from known functions in other organisms.

2.4 *RNA-Seq, Qualitative, and QPCR Expression Analyses*

We evaluated genes located within predicted critical genomic regions for expression differences using RNA-seq. Total RNA was isolated from pools of 50 surface or cave individuals using the RNeasy Plus Mini Kit (Qiagen) at each of five developmental stages. These included 10 hours post-fertilization (hpf), 24, 36, and 72 hpf, and from three individuals during juvenilehood (~4 months). Library preparation (TruSeq v.2 kit) and sequencing (Illumina 2500 Hi-Seq) was performed in triplicate (10–72 hpf) or duplicate (juvenile) at the DNA Sequencing Core (Cincinnati Children's Hospital and Medical Center). All samples were sequenced to a ~10 million read depth for 50-bp, single-end reads. Normalized gene expression was calculated using ArrayStar (DNAStar). All expressions were evaluated using comparative read counts between cave and surface fish with the RPKM normalization method (Mortazavi et al. 2008). Raw sequencing reads are deposited at the NCBI SRA (BioProject: PRJNA258661).

We validated expression profiles at the 72 hpf stage using qualitative and quantitative PCR analyses, described in Stahl and Gross (2017). Template cDNA from surface and cavefish RNA pools (n = 50 embryos each; RNeasy Plus Mini kit, Qiagen) was synthesized for both experiments using the Transcriptor RT kit (Roche). Quantitative PCR (qPCR) experiments were performed as described in Stahl and Gross (2017). All samples were analyzed in sextuplet and normalized expression values (C_q) and significant differences (two-tailed Student's t-test) were determined using the CFX Manager software program (v.3.1; BioRad).

Genes residing within the syntenic region in the *Astyanax* genome were analyzed for sequence alterations. Sequencing reads derived from surface fish and Pachón cavefish (~280 million reads total) were aligned to the draft *Astyanax* genome (Ensembl.v.75; McGaugh et al. 2014) using default parameters for the program Seq-Man NGen (DNASTAR) and evaluated for diverse sequence mutations (e.g., SNP, indels) segregating between surface and cave morphs.

2.5 Whole-Mount In Situ Hybridization

RNA probes for in situ hybridization were generated by PCR for the genes *Tyrp1b* (forward primer: 5′-GAAACAGCCCTCAGTTCGAG-3′, reverse primer: 5′-AGGTGGGCCAGATTGTGTAG-3′) and *Pmela* (forward primer: 5′-CTACTGATGCTGCCACTGGA-3′, reverse primer: 5′-AGAGCCGTAGCGGTAGATCA-3′). The resulting PCR products were cloned into the TOPO TA Dual Promoter cloning vector (Life Technologies) and confirmed by sequencing. Sense and antisense digoxygenin (DIG)-labeled RNA probes for *Astyanax Tyrp1b* and *Pmela* were transcribed with either SP6 or T7 RNA polymerase (Roche). Whole-mount in situ hybridizations were performed on embryos at stages <12 hours post-fertilization (hpf), 24, 36, and 72 hpf according to Ma et al. (2014). Embryos were washed in NTM, PBT, and TBST and fixed in 4% PFA/PBS for storage at 4 °C and visualized using Leica Microscope M205 FA (with LAS software v.3.8.0) montage imaging (Fig. 5a–d). The numbers of cells with positive expression for *Pmela* or *Tyrp1b*, respectively, were counted.

2.6 Functional Validation in Zebrafish with MO Knockdowns

The translational blocking morpholino oligonucleotides were targeted to the first 25 base pairs of the zebrafish ORF of *Pmela* (5′-GAGGAAGATGAGAGATGTCCACAT-3′) and *Tyrp1b* (5′-GCACTAAACACACACTCTTCCACAT-3′; Gene Tools, LLC.). Morpholinos were injected into one-cell stage zebrafish embryos in a 1 nl volume at a 0.2 mM concentration. Control individuals were administered a mock injection composed of phenol red and Danieaux's solution (Wingert et al. 2004), or a control oligo (5′-CCTCTTACCTCAGTTACAATTTATA-3′; Gene Tools, LLC). Imaging was performed using a Leica Microscope M205 FA (with LAS software v.3.8.0) stereo-scope (Fig. 5e–g). Phenotypic analysis was performed on embryos fixed at 5dpf in 4% PFA. Counts were performed on the yolk sac of the number of light and dark melanophores, and the number of clustered and isolated melanophores, both relative to total melanophore number on the yolk sac (Fig. 5h, i).

3   Results

3.1   *Cavefish* × *Surface Fish Hybrid Individuals Demonstrate Diversity in Melanophore Numbers in Distinct Regions Spanning the Body*

Direct observations reveal a wide array of pigmentation variation among F_2 siblings (Fig. 1a–e), and substantial pigment cell variation has been reported in four different body regions (Protas et al. 2007). We quantified melanophore number in seven areas and found variation across our F_2 population (n = 170). Counts ranged within each region (reported as minimum to max number melanophore distribution for a given region among the entire F_2 pedigree): 1–99 melanophores in the square near the anal fin (MelAnalfinSquare), 1–113 pigment cells below the mid-lateral stripe (MelUnderStripe), 4–600 cells in the dorsal square (MelDorsalSquare), 1–2,762 melanophores in the area above the stripe (MelAboveStripe), 1–89 pigment cells above the eye (MelHeadSquare), 11–1,395 melanophores present in the full head region (MelHead), and 0–252 pigment cells by the anal fin (MelAnalfinTriangle). Numerical variation in melanophore numbers did not simply increase or decrease proportionately across all regions of the body, instead pigment cell numbers in some cases varied independently between different assayed regions.

3.2   *QTL Analysis Revealed 19 Genomic Regions Associated with Complex Melanophore Variation*

We scored melanophore variation in seven regions and detected numerous QTL (Fig. 2a). We did not discover QTL for melanophores on the entire head (MelHead). This was surprising since we detected QTL for pigment cell counts in the head square above the eye (MelHeadSquare). Additionally using four different mapping methods, our results yielded multiple significant (independent) associations (n = 41 markers) with the linkage map for the following pigment cell number traits: MelAnalfinSquare (n = 1 QTL), MelUnderStripe (n = 13 QTL; Fig. 2d, e), MelDorsalSquare (n = 3 QTL; Fig. 2b, c), MelAboveStripe (n = 1 QTL), MelHeadSquare (n = 3 QTL), and MelAnalfinTriangle (n = 6 QTL). In some instances, the different mapping methods identified significant associations with same top marker (e.g., MR, EM, HK, and NP methods all noted the marker ASTYANAX_414 at single map location (LG 16, 22.2 cM for MelUnderStripe), and in other cases, the different approaches yielded multiple significant markers within a small positional window—for example, three-markers for each MR, EM, and HK respective method for MelDorsalSquare on LG 20 (53–61 cM). Not surprisingly, some of these QTL co-localized near the same position in our linkage map. One "hotspot" in our map was on linkage group 1 from 75 to 93 cM, wherein associations with five traits (MelHeadSquare, MelUnder-
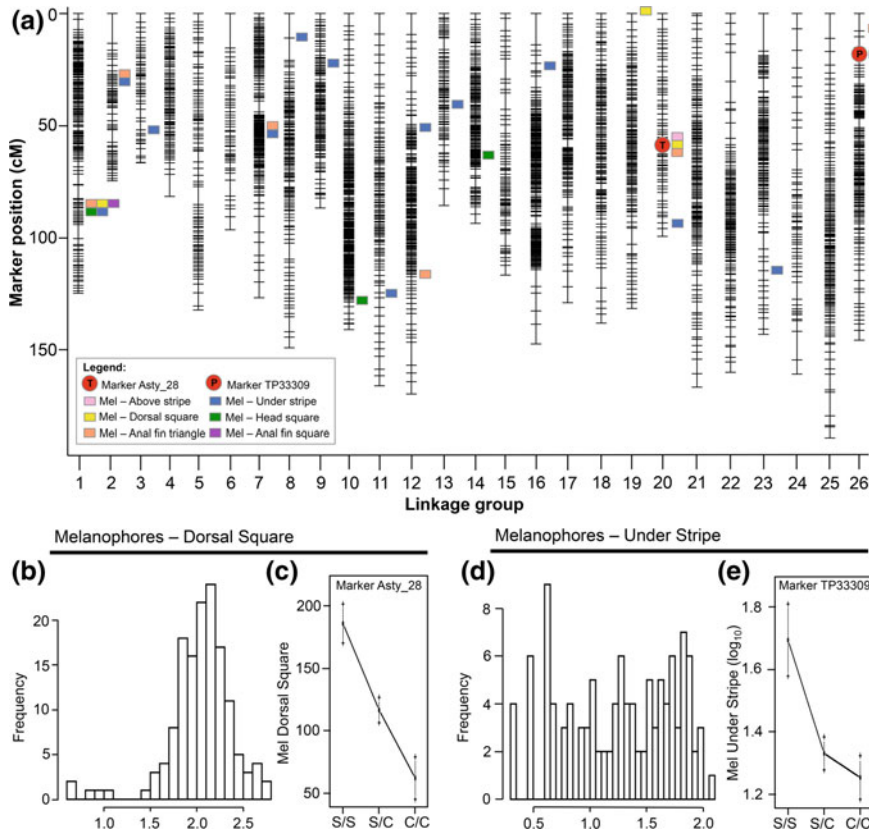
Fig. 2 High-resolution mapping identified multiple QTL associations with melanophore number variation. Our quantitative trait locus (QTL) study detected numerous associations (n = 40) with pigment cell variation (**a**). Many of these co-localized to similar positions on our linkage map. With this approach, we were able to capture the dramatic variation of pigment cell number, including the range of melanophores detected in the dorsal square (**b**) and under the mid-lateral stripe (**d**). The frequency denotes the number of individuals harboring a given number of melanophores. The markers underlying these two QTL demonstrated a significant effect of phenotype, where individuals harboring two copies of the surface allele "S/S" demonstrated increased numbers of melanophores, and hybrids with two cavefish alleles "C/C" exhibited fewer pigment cells. This effect is evident in both the dorsal (**c**) and stripe (**e**) regions assayed

Stripe, MelAnalfinTriangle, MelDorsalSquare, MelAnalfinSquare) yielded significant QTL (Fig. 2a). Moreover, three different regions assayed (MelDorsalSquare, MelAnalfinTriangle, MelAboveStripe) returned associations with linkage group (LG) 20 (53–61 cM), and two traits (MelAnalfinTriangle, MelUnderStripe) tended to co-localize together at several positions: LG 2 (29.8–33.6 cM), LG 7 (54.64–63.7 cM) and LG 26 (8.98–18 cM). In total, we discovered 19 distinct regions (QTLs) of the genome are associated with melanophore variation (Fig. 2a).

3.3 *Comparative Analyses Narrowed Melanophore QTL Positions to Critical Genomic Regions in* Astyanax *and* Danio

To further search for candidate genes residing near our top markers, we analyzed the positions of each QTL in the *Astyanax* cavefish draft genome (~10,000 scaffolds) and the current zebrafish genome (Ensembl.Zv9). First, we queried marker sequences to the *Astyanax* genome (Ensembl.v.75) using the standard nucleotide BLAST algorithm to find the position of the top genomic marker, and the locations of the markers within the QTL interval (immediately adjacent ~6–8 cM to the top marker), to identify regions of synteny. Since these scaffolds varied in length (876–9,823,298 bp), the number of scaffolds reported back from our BLAST search ranged from 4 to 27 scaffolds for each association (data not shown).

We also capitalized on the well-annotated genome of teleost fish *Danio rerio*. Three comparative studies previously identified large syntenic regions shared between *Astyanax* and *Danio*, which diverged ~120 MYa (Gross et al. 2008; Gross 2012b; O'Quin et al. 2013; Carlson et al. 2015). Our genomic comparisons revealed several syntenic blocks based on the positions of BLAST hits in *Danio*, yielding regions of synteny on different zebrafish chromosomes. We sought to further support the syntenic block from our direct comparisons of marker sequences to zebrafish, since usually <20 markers yielded direct BLAST hits for each QTL. Accordingly, we collected every predicted gene (often 100+ genes) from the respective *Astyanax* scaffolds associated with each QTL and queried the full-length gene sequences to the zebrafish genome.

3.4 *Tyrp1b* and *Pmela* *Are Two Candidate Genes Associated with Numerical Melanophore Diversity*

Nearly all of the assayed pigmentation traits yielded multiple QTL associated with multiple distinct regions of the linkage map (Fig. 2a). We characterized the wide range of melanophore number variation in our pedigree, including the dorsal square (Fig. 2b) and inferior to the mid-lateral stripe (Fig. 2d). Our association studies revealed multiple loci for these traits, including the markers ASTYANAX_28 on LG 20 (LOD[MR] = 6.01, p = 0.015) and TP33309 on LG 26 (LOD[MR] = 5.08, p = 0.041), respectively (see red circles in Fig. 2a). Corresponding effect plots demonstrated a significant effect of genotype for each marker: homozygous surface alleles "S/S" harbor more melanophores and homozygous cave alleles "C/C" have fewer melanophores (Fig. 2c, e). The heterozygous genotype for ASTYANAX_28 presented an intermediate number of melanophores at this locus, whereas the heterozygous genotype at TP33309 has melanophore numbers similar to the homozygous cave genotype, perhaps indicating the dominance of the cave allele in hybrid individuals.

To pursue candidate genes, we collected the ontology for genes within the syntenic blocks. For the QTL association on LG 20 (marker: ASTYANAX_28), we identified 951 terms affiliated with 157 genes on 10 *Astyanax* scaffolds, and 868 terms associated with 193 genes from the syntenic interval anchoring to chromosome 1 in zebrafish. Within this dataset, we identified two GO terms related to pigmentation: "melanosome membrane" (GO:0033162) and "melanin biosynthetic process" (GO:0042438) of which both terms are associated with two genes *Tyrp1b* and *Tyrp1a* in *Astyanax,* and "pigmentation" (GO:0043473) with the gene *Tyrp1b* in the zebrafish syntenic block. We note that the *Tyrp1a* paralog resides on a different chromosome (Chr7) in *Danio rerio,* whereas *Tyrp1b* resides on chromosome 1 in zebrafish, (described above). Additionally, we discovered 1,136 GO terms for 409 genes associated with 12 scaffolds for "MelUnderStripe" on LG 26 (marker: TP33309), and 3,017 terms for the 654 genes within the critical block on chromosome 11 in *Danio rerio.* This analysis revealed three pigmentation GO terms in *Astyanax* including "melanosome transport" (GO:0032402) linked to *Ippk* and "developmental pigmentation" (GO:0048066) and "eye pigmentation" (GO:0048069) assigned to *Pmela*. In *Danio*, we identified "developmental pigmentation" (GO:0048066) and "eye pigmentation" (GO:0048069) associated with *Pmela*. By co-analyzing gene ontology and positional information from both organisms, we nominated candidate genes for each QTL: *Tyrp1b* (LG20) and *Pmela* (LG26). These two genes reside in close proximity to the top two QTL markers, ~7 MB and ~0.05 MB, respectively (Fig. 3a, d).

Next, we interrogated the coding sequences by aligning surface- and cave-tagged RNA sequencing reads to the *Astyanax* draft genome. *Tyrp1b,* near a marker where multiple melanophore traits were mapped, harbored three mutations, including a G-to-A substitution in exon 2 at position 630 (Fig. 3b). This is predicted to be a synonymous change (F210F); however, it falls within a tyrosinase copper-binding domain (205–222 bp; Ensembl.v.75) which could affect interactions with tyrosinase—an enzyme catalyzing melanin biosynthesis (Oetting 2000). Synonymous mutations such as these can affect splicing, stability, structure, and protein folding (Hunt et al. 2009). For the gene *Pmela*, sequence analyses revealed numerous alterations, such as a G-to-A change at position 1738 in exon 7 (Fig. 3e). This non-synonymous mutation impacts the amino acid sequence, causing a change from a hydrophobic alanine residue to a hydrophilic threonine in cavefish (A580T). In addition, *Pmela* demonstrates several more mutations including two other non-synonymous changes, two silent SNPs, and three potential splice variants.

With respect to expression, *Tyrp1b* showed reduced expression in cave relative to surface beginning at 24 hpf (Fig. 3c). We observed expression differences of 7-fold down (36 hpf) and 5.5-fold down (72 hpf; Fig. 3c). Expression profiles of cave versus surface forms demonstrated significant differences at 10 hpf ($p = 0.0472$), 36 hpf ($p = 0.0312$), and 72 hpf ($p = 0.00167$). *Pmela* similarly revealed reduced expression at 24 hpf (Fig. 3f). *Pmela* demonstrated a 12-fold reduction in expression at 72 hpf. Levels of gene expression were significantly different between morphs at four stages assayed: 10 hpf ($p = 0.00607$), 24 hpf ($p = 0.00117$), 36 hpf ($p = 0.0311$), and 72 hpf ($p = 0.000239$). Using qualitative and quantitative PCR, we observed weaker bands
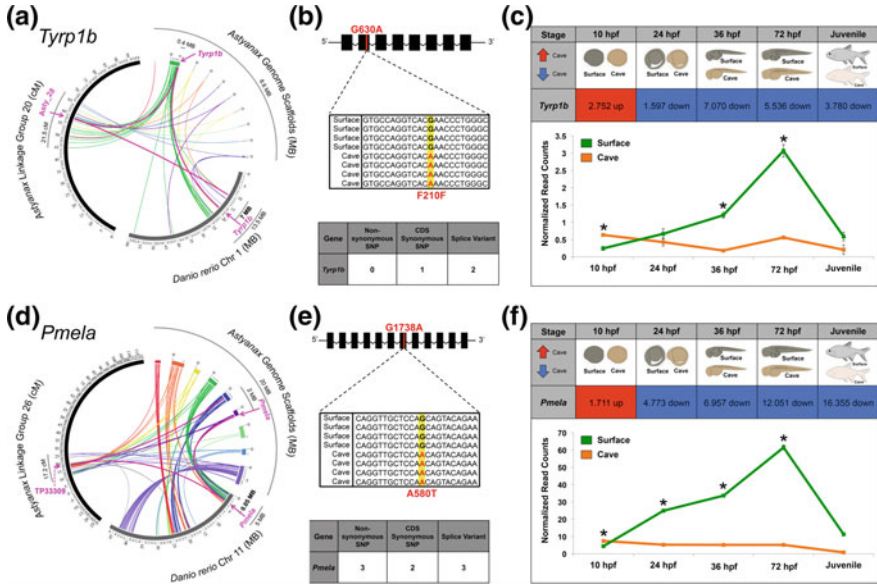
Fig. 3 Integrative analyses reveal two candidate genes for melanophore variation. The evaluation of melanophore variation using QTL analyses identified two top candidate genes that may be associated with pigmentation loss in *Astyanax mexicanus* cavefish. Pigment cell variation under the mid-dorsal stripe region showed a significant association with marker ASTYANAX_28 on LG 20 (LOD^{MR} = 6.01, p = 0.015), which anchors to genomic regions in *Astyanax* and *Danio* inclusive of *Tyrosinase-related protein 1b* (*Tyrp1b*; **a**). Distances between the top marker and candidate gene are in boldface. A second melanophore trait in the superior dorsal region demonstrates a significant association with marker TP33309 on linkage group 26 (LOD^{MR} = 5.08, p = 0.041; **d**). Regions of synteny were identified between *Astyanax* and *Danio rerio*. The syntenic region was mined for any genes with potential roles in the pigmentation pathway using gene ontology (GO) terms. This led to the discovery of the gene *Premelanosome protein a (Pmela)*. These two candidates, and any other pigment-related genes that exist within the syntenic region, were evaluated for prospective coding mutations and expression alterations using RNA-seq technologies (**b–c**, **e–f**). This combined approach has led to discovery of candidate genes that may contribute to loss of pigmentation in cave-dwelling fish

in Pachón cavefish compared to the surface fish for *Tyrp1b* and *Pmela* (gel images not shown), and significantly reduced expression in Pachón cavefish for *Tyrp1b* (p = 0.005967; Fig. 4a, c) and *Pmela* (p < 0.000001; Fig. 4b, d).
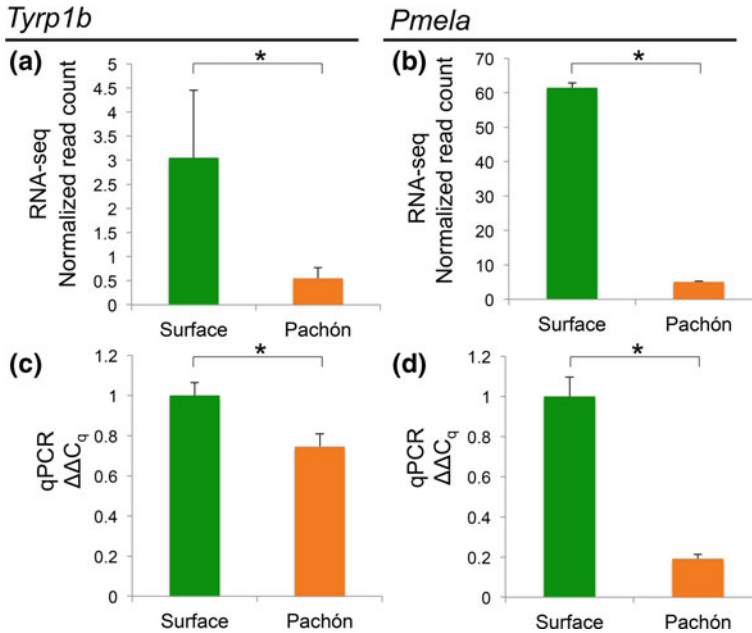
Fig. 4 Quantitative (qPCR) confirms reduced expression of *Tyrp1b* and *Pmela* in Pachón cavefish. To further validate reduced expression patterns from our RNA-seq expression profiling (**a**, **b**), we performed quantitative PCR on surface and Pachón cavefish at 72 hpf. These analyses confirmed dramatic reduction of expression in cave-dwelling morphotypes for both *Tyrp1b* (p = 0.005967) and *Pmela* (p < 0.000001)

3.5 **Tyrp1b** *and* **Pmela** *Demonstrate Distinct Melanophore-Specific Expression Patterns Between Cave and Surface Morphotypes*

Both *Pmela* and *Tyrp1b* appear to influence both melanophore position and melanin density in *A. mexicanus* and *D. rerio* (Fig. 5). Analysis of the location of *Pmela* (Fig. 5a, b) and *Tyrp1b* (Fig. 5c, d) gene expression following in situ hybridization indicates a heterochronic delay in cavefish compared to surface fish. Early in development (<12 hpf), *Pmela* and *Tyrp1b* gene expressions are apparent in more cells in surface fish than in cavefish. Later in development, surface fish exhibits higher numbers of cells with positive *Pmela* expression posteriorly than cavefish.
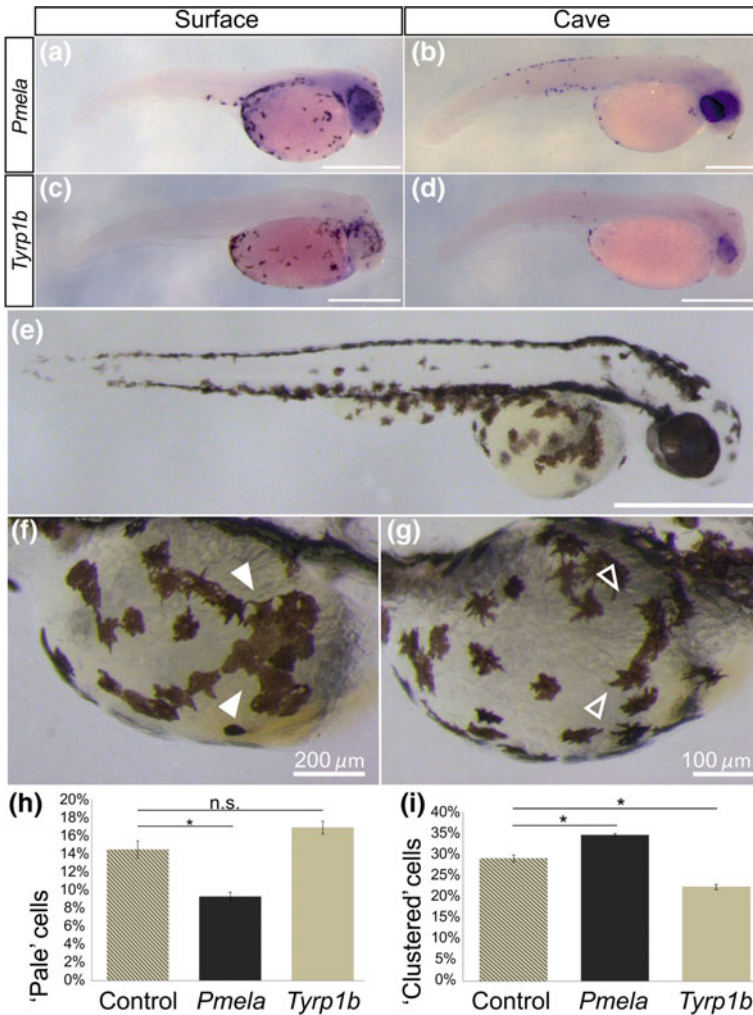
Fig. 5 Expression and functional analysis of *Pmela* and *Tyrp1b* candidate genes. In situ hybridization of *Pmela* (**a**, **b**) and *Tyrp1b* (**c**, **d**) of cave (**b**, **d**) and surface fish (**a**, **c**) embryos. At this stage, surface fish embryos have begun to develop melanin pigmentation across the yolk sac and putative eye regions, which appears to coincide with *Tyrp1b* and *Pmela* gene expression. In individuals stained for *Pmela,* we see a difference in spatial distribution of gene expression between cave and surface embryos. Morpholino knockdown of 5dpf *D. rerio* embryos (**e–g**). The control-injected (**e**) embryos display a "normative" melanophore distribution and density in comparison to *Pmela* (**f**) and *Tyrp1b* (**g**) knockdowns. **f** Filled arrowheads show clustering of melanophores in *Pmela* morphants. (**g**) Open arrowheads show a higher dispersal of melanophores in *Tyrp1b* morphants. A total number of melanophores on the yolk sac were counted to determine the ratio of pale (**h**) or clustered (**i**) melanophores. *Pmela* knockdowns exhibit a clustering of melanophores across the yolk sac ($p < 0.05$) and a lesser ratio of "pale" melanophores ($p < 0.05$) than control-injected embryos. (**i**) *Tyrp1b* knockdowns have a higher distribution of melanophores across the yolk sac ($p < 0.05$) and a higher number of "pale" melanophores (n.s.) than control. Scale bars at 500 µm, unless otherwise noted

3.6   Functional Analyses of **Tyrp1b** and **Pmela** Reveal Altered Melanophore Dispersion and Structure in Morphants

We utilized the closely related (120 MYa diverged), and laboratory-established fish species *Danio rerio,* to carry out morpholino experiments (Fig. 5e–g). *Pmela* knockdown via MO injection resulted in clustering of melanophores across the yolk sac (Fig. 5f, i), coincident with a lesser number of pale melanophores (Fig. 5h). In contrast to *Pmela* morphants, *Tyrp1b* morphants have a higher number of pale cells compared to control individuals (Fig. 5h). This corresponds to the wider dispersal of melanophores (Fig. 5g) and a higher number of "pale" melanophores on the yolk sac of *Tyrp1b* morphants. Both *Pmela* and *Tyrp1b* appear to influence melanophore darkness and position, based upon phenotypes of *D. rerio* morphants.

4   Discussion

4.1   **Tyrp1b** and **Pmela** Contribute to Melanophore Number Variation in Cavefish

Cave-dwelling *Astyanax* has evolved diverse phenotypes upon colonization of the cave, including a reduction in pigmentation and eyes, and character expansion of taste and touch sensation (Montgomery et al. 2001; Gross 2012a; Kowalko et al. 2013). Here, we utilized an integrative approach to identify two genes—*Tyrp1b* and *Pmela*—that play a role in complex melanophore number diversity in *Astyanax*. In *Astyanax*, deeply conserved sets of pigmentation-related processes may be governed by *Tyrp1b* and *Pmela*. *Tyrp1* serves as a stabilizing protein for tyrosinase which functions in melanin production, and when the *Tyrp1b* protein is absent, tyrosinase rapidly degrades (Müller et al. 1988; Kobayashi and Hearing 2007). In mice, two distinct *Tyrp1* alleles in transgenic mice yield degenerative pigmentation: one causing brown coat coloration or nearly white fur relative to the normally black mice (*b* allele), and another form that could induce albinism (*c* allele; Kwon et al. 1989). Similarly, variants of *Tyrp1* are the cause of "chocolate" and "cinnamon" coat colors in the domestic cat (Lyons et al. 2005; Schmidt-Küntzel et al. 2005). Numerous *Tyrp* alleles have also been identified in humans as a cause of oculocutaneous albinism type III, which are often caused by small deletions or single base pair changes impacting the amino acid sequence (Forshew et al. 2005; Rooryck et al. 2006; Chiang et al. 2008; Kenny et al. 2012).

While most mutations in *Tyrp1* are the result of non-synonymous changes, we discovered a synonymous alteration in the coding sequence (F210F; Fig. 3b). Some studies of *Tyrp1b* also include synonymous mutations (e.g., six silent SNPs in the domestic cat) for which the precise impact has not yet been explained (Lyons et al. 2005).

Our RNA-seq and qPCR studies indicated significantly reduced *Tyrp1b* expression in Pachón cavefish compared to the surface-dwelling form. The reduced expression in cavefish may contribute to instability of tyrosinase and may be responsible, in part, for the reduced numbers of melanophores observed in Pachón cave morphotypes.

The gene *Pmela* which is also known as "*Silv*" or "*Pmel17*" is a similarly well-described gene associated with pigmentation (Theos et al. 2005). This gene is responsible for recessive dilution of coat color that deteriorates with age in inbred mouse strains (Dunn and Thigpen 1930). Variants of *Pmela* cause dilution or hypotrichosis of coat color in the domestic yak (Zhang et al. 2014), cattle (Jolly et al. 2011; Schmutz and Dreger 2013), and the "silver" phenotypes in horse (Brunberg et al. 2006) and zebrafish (Schonthaler et al. 2005).

We discovered three non-synonymous changes to the *Pmela* coding sequence, including G580A in cavefish, which causes an alanine-to-threonine substitution. This is intriguing since *Pmela* undergoes posttranslational modification and processing imperative for proper functioning (Theos et al. 2013). The change from a hydrophobic alanine (nonpolar side chains) to a hydrophilic threonine (polar side chains) may alter the Pmela protein. Ala-to-Thr residue changes in diverse proteins have been shown to induce self-aggregation into amyloids (i.e., an insoluble β-pleated sheet formed by the alteration in secondary structure). Although some amyloids are native to Pmel, additional changes in this structure-sensitive protein may impact normal functioning (Fowler et al. 2005).

Pmela has been described as a melanocyte-specific type 1 transmembrane encoded protein enriched in melanosomes (i.e., the pigment-producing organelles within the melanocytes/melanophores; reviewed in Theos et al. 2005). The gene *Pmela* plays a critical role in the premelanosome "fibril" ultrastructure, and Pmel-targeted antibodies are evident in fibrous, stage II melanosomes as Pmel is thought to polymerize fibrillar arrays that ultimately form the backbone of eumelanosomes (Spanakis et al. 1992; Solano et al. 2000; Raposo et al. 2001; Berson et al. 2001; Raposo and Marks 2002). Moreover, high levels of *Pmela* expression in non-agouti (solid dark) mice are necessary to construct the fibrils associated with the shape of eumelanosomes (Theos et al. 2005).

We detected the substantial reduction in *Pmela* expression across early development in Pachón cavefish relative to surface fish. Reduced *Pmela* expression could impede fibril formation, leading to the aberrant melanophore morphology observed in our knockdown studies. Other reports similarly describe changes in melanosome shape but modest effects on overall body pigmentation in mice (Hellström et al. 2011). *Pmela* mutants often have reduced or scattered pigment granules in individual hairs (Dunn and Thigpen 1930). Furthermore, the "merle" phenotype in domestic dogs (e.g., Australian shepherds) is caused by codominance of the merle (M) and non-merle (m) *Pmel* alleles in heterozygous individuals that collectively yield patches of dark and light-colored fur due to spatially random protein instability (Clark et al. 2006; Schmutz and Berryere 2007). These degenerative pigmentation phenotypes, combined with the structural changes and severely reduced expression in colorless cavefish, suggest that *Tyrp1b* and *Pmela* contribute to the complex trait of melanophore variation in *Astyanax mexicanus*.

4.2   Analysis of Complex Pigmentation Informs the Genetic Basis for Regressive Evolution in Cavefish

Three hypotheses seeking to explain regressive evolution include natural selection, neutral mutation/genetic drift, and pleiotropy (Culver 1982). A prior QTL study yielded 18 loci associated with numerical melanophore variation. In certain cases, the homozygous cave genotype was associated with *increased* numbers of melanophores (Protas et al. 2007). Our study revealed a similar result—genotypic effect plots varied in their polarity for members our experimental F_2 pedigree. This may provide evidence for neutral mutation/genetic drift since it would be unlikely that depigmented cavefish (if under selection) would harbor alleles that increase pigment cell number (Protas et al. 2007). However, one potential "selective" benefit for loss of pigmentation in cave-dwelling morphs may be activation of the catecholamine pathway to encourage foraging behavior in the nutrient-poor subterranean environment (Bilandžija et al. 2013). Although the precise evolutionary pressures governing regression remain unknown, further studies will reveal the genetic mechanisms accompanying trait loss in the wild.

4.3   Astyanax mexicanus *Enables Investigation of Degenerative Pigmentation Disorders*

Degenerative pigmentation can be found widely around the globe, including clinical diseases impacting humans such as albinism, vitiligo, and skin melanoma (Oetting et al. 1996; Agarwal 1998; Hocker and Tsao 2007). Often the etiologies for these disorders remain unknown. Animals that naturally demonstrate degenerative traits, such as the blind Mexican cavefish, can help understand pigmentation losses since they have recurrently evolved extreme pigmentation changes as a consequence of the extreme cave environment (Jeffery 2005; Gross 2012a). Since the functions of many pigmentation genes are shared broadly across taxa, we can make progress toward understanding the comprehensive role of novel genes in the regulation of animal pigmentation, including albinism (Protas et al. 2005) and *brown* (Valverde et al. 1995; Flanagan et al. 2000; Rees 2003).

Here, we suggest a role for *Tyrp1b* and *Pmela* in melanophore variation in cavefish, and these genes are also critical for the normal production of melanin in humans. For instance, in humans, *Tyrp1* is responsible for oculocutaneous albinism type III due to coding sequence alterations. In cavefish, *Tyrp1* has been repeatedly mutated, including alleles associated with different geographic regions (Manga et al. 1997; Forshew et al. 2005; Rooryck et al. 2006). However, more common *Tyrp1* alleles contribute to normal hair, skin, and iris variation in humans (Frudakis et al. 2003; Sulem et al. 2008; Han et al. 2008; Liu and Fisher 2010; Eriksson et al. 2010). Our knowledge of *Pmela* variants in humans is more limited, and some of the disorders present in other animals (e.g., double merle dogs) also cause hearing and ocular defi-

ciencies due to pigmentation losses in the ears and eyes (Clark et al. 2006). Evaluation of pigmentation genes in cavefish will continue to identify vulnerable genes, shared broadly across taxa that may improve our knowledge of human, pigmentation-related diseases.

Ethical Statement All applicable international, national, and/or institutional guidelines for the care and use of animals were followed. All procedures performed in studies involving animals were in accordance with the ethical standards of the institution or practice at which the studies were conducted. The protocol was approved by the Institutional Animal Care and Use Committee (IACUC) of the University of Cincinnati (Protocol Number 10-01-21-01).

References

Agarwal GA (1998) Vitiligo: an under-estimated problem. Fam Pract 15(Suppl 1):S19–23

Berson JF, Harper DC, Tenza D, Raposo G, Marks MS (2001) *Pmel17* initiates premelanosome morphogenesis within multivesicular bodies. Mol Biol Cell 12:3451–3464

Bilandžija H, Ma L, Parkhurst A, Jeffery WR (2013) A potential benefit of albinism in *Astyanax* cavefish: Downregulation of the *oca2* gene increases tyrosine and catecholamine levels as an alternative to melanin synthesis. PLoS ONE 8:e80823-14

Borowsky R (2008) *Astyanax mexicanus*, the blind Mexican cave fish: a model for studies in development and morphology. Cold Spring Harbor Protocols 2008:pdb.emo107

Broman KW, Wu H, Sen Ś, Churchill GA (2003) R/qtl: QTL mapping in experimental crosses. Bioinformatics 19:889–890

Brunberg E, Anderson L, Cothran G, Sandberg K, Mikko S, Lindgren G (2006) A missense mutation in *PMEL17* is associated with the Silver coat color in the horse. BMC Genet 7:46

Carlson BM, Onusko SW, Gross JB (2015) A high-density linkage map for *Astyanax mexicanus* using genotyping-by-sequencing technology. G3: Genes Genomes Genet 5:241–251

Chiang PW, Fulton AB, Spector E, Hisama FM (2008) Synergistic interaction of the *OCA2* and *OCA3* genes in a family. Am J Med Genet Part A 146A:2427–2430

Clark LA, Wahl JM, Rees CA, Murphy KE (2006) Retrotransposon insertion in *SILV* is responsible for merle patterning of the domestic dog. Proc Natl Acad Sci 103:1376–1381

Culver DC (1982) Cave life: evolution and ecology. Harvard University Press, Cambridge, 189 pp

Dunn LC, Thigpen LW (1930) The silver mouse: a recessive color variation. J Hered 21:495–498

Erickson CA, Perris R (1993) The role of cell-cell and cell-matrix interactions in the morphogenesis of the neural crest. Dev Biol 159:60–74

Eriksson N, Macpherson JM, Tung JY, Hon LS, Naughton B, Saxonov S, Avey L, Wojcicki A, Pe'er I, Mountain J (2010) Web-based, participant-driven studies yield novel genetic associations for common traits. PLoS Genet 6:e1000993

Flanagan N, Healy E, Ray A, Philips S, Todd C, Jackson IJ, Birch-Machin MA, Rees JL (2000) Pleiotropic effects of the melanocortin 1 receptor (*Mc1r*) gene on human pigmentation. Hum Mol Genet 9:2531–2537

Forshew T, Khaliq S, Tee L, Smith U, Johnson CA, Mehdi SQ, Maker ER (2005) Identification of novel *TYR* and *TYRP1* mutations in oculocutaneous albinism. Clin Genet 68:182–184

Fowler DM, Koulov AV, Alory-Jost C, Marks MS, Balch WE, Kelly JW (2005) Functional amyloid formation within mammalian tissue. PLoS Biol 4:e6

Frudakis T, Thomas M, Gaskin Z, Venkateswarlu K, Chandra KS, Ginjupalli S, Gunturi S, Natrajan S, Ponnuswamy VK, Ponnuswamy KN (2003) Sequences associated with human iris pigmentation. Genetics 165:2071–2083

Gross JB (2012a) Cave evolution. In: Encyclopedia of life sciences, eLS. Wiley

Gross JB (2012b) The complex origin of *Astyanax* cavefish. BMC Evol Biol 12:105–122

Gross JB, Wilkens H (2013) Albinism in phylogenetically and geographically distinct populations of *Astyanax* cavefish arises through the same loss-of-function *Oca2* allele. Heredity 111:122

Gross JB, Borowsky R, Tabin CJ (2009) A novel role for *Mc1r* in the parallel evolution of depigmentation in independent populations of the cavefish *Astyanax mexicanus*. PLoS Genet 5:e1000326-14

Gross JB, Protas ME, Conrad M, Scheid PE, Vidal O, Jeffery WR, Borowsky R, Tabin CJ (2008) Synteny and candidate gene prediction using an anchored linkage map of *Astyanax mexicanus*. Proc Natl Acad Sci 105:20106–20111

Gross JB, Krutzler AJ, Carlson BM (2014) Complex craniofacial changes in blind cave-dwelling fish are mediated by genetically symmetric and asymmetric loci. Genetics 196:1303–1319

Haley CS, Knott SA (1992) A simple regression method for mapping quantitative trait loci in line crosses using flanking markers. Heredity 69:315–324

Han J, Kraft P, Nan H, Guo Q, Chen C, Qureshi A, Hankinson SE, Hu FB, Duffy DL, Zhao ZZ, Martin NG, Montgomery GW, Hayward NK, Thomas G, Hoover RN, Chanock S, Hunter DJ (2008) A genome-wide association study identified novel alleles associated with hair color and skin pigmentation. PLoS Genet 4:e1000074

Hellström AR, Watt B, Fard SS, Tenza D, Mannström P, Mannström K, Ekesten B, Ito S, Wakamatso K, Larsson J, Ulfendahl M, Kullander K, Raposo G, Kerje S, Hallböök F, Marks MS, Andersson L (2011) Inactivation of *Pmel* alters melanosome shape but has only a subtle effect on visible pigmentation. PLoS Genet 7:e1002285

Hocker T, Tsao H (2007) Ultraviolet radiation and melanoma: a systematic review and analysis of reported sequence variants. Hum Mutat 28:578–588

Hoekstra HE (2006) Genetics, development and evolution of adaptive pigmentation in vertebrates. Heredity 97:222–234

Huang X, Saint-Jeannet JP (2004) Induction of the neural crest and the opportunities of life on the edge. Dev Biol 275:1–11

Hubbard JK, Uy JAC, Hauber ME, Hoekstra HE, Safran RJ (2010) Vertebrate pigmentation: from underlying genes to adaptive function. Trends Genet 26:231–239

Hunt R, Sauna ZE, Ambudkar SV, Gottesman MM, Kimchi-Sarfaty C (2009) Silent (synonymous) SNPs: should we care about them? Single nucleotide polymorphisms. Humana Press, Totowa, NJ, pp 23–29

Jeffery WR (2001) Cavefish as a model system in evolutionary developmental biology. Dev Biol 231:1–12

Jeffery WR (2005) Adaptive evolution of eye degeneration in the Mexican blind cavefish. J Hered 96:185–196

Jeffery WR (2006) Regressive evolution of pigmentation in the cavefish *Astyanax*. Isr J Ecol Evolut 52:405–422

Jeffery WR (2009) Evolution and development in the cavefish *Astyanax*. Curr Top Dev Biol 86:191–221

Jolly RD, Wills JL, Kenny JE, Cahill JI, Howe L (2011) Coat-colour dilution and hypotrichosis in Hereford crossbred calves. N Z Vet J 56:74–77

Kasprzyk A (2011) BioMart: driving a paradigm change in biological data management. Database 2011:bar049

Kearsey MJ, Hyne V (1994) QTL analysis: a simple "marker-regression" approach. Theor Appl Genet 89:698–702

Kenny EE, Timpson NJ, Sikora M, Yee M-C, Moreno-Estrada A, Eng C, Huntsman S, González Burchard E, Stoneking M, Bustamante CD, Myles S (2012) Melanesian blond hair is caused by an amino acid change in *TYRP1*. Science 336:554–554

Klaassen H, Wang Y, Adamski K, Rohner N, Kowalko JE (2018) CRISPR mutagenesis confirms the role of *oca2* in melanin pigmentation in *Astyanax mexicanus*. Dev Biol (in press). https://doi.org/10.1016/j.ydbio.2018.03.014

Kobayashi T, Hearing VJ (2007) Direct interaction of tyrosinase with *Tyrp1* to form heterodimeric complexes *in vivo*. J Cell Sci 120:4261–4268

Kowalko JE, Rohner N, Linden TA, Rompani SB, Warren WC, Borowsky R, Tabin CJ, Jeffery WR, Yoshizawa M (2013) Convergence in feeding posture occurs through different genetic loci in independently evolved cave populations of *Astyanax mexicanus*. Proc Natl Acad Sci 110:16933–16938

Kruglyak L, Lander ES (1995) A nonparametric approach for mapping quantitative trait loci. Genetics 139:1421–1428

Krzywinski M, Schein J, Birol I, Connors J, Gascoyne R, Horsman D, Jones SJ, Marra MA (2009) Circos: an information aesthetic for comparative genomics. Genome Res 19:1639–1645

Kwon BS, Halaban R, Chintamaneni C (1989) Molecular basis of mouse Himalayan mutation. Biochem Biophys Res Commun 161:252–260

Linnen CR, Kingsley EP, Jensen JD, Hoekstra HE (2009) On the origin and spread of an adaptive allele in deer mice. Science 325:1095–1098

Liu JJ, Fisher DE (2010) Lighting a path to pigmentation: mechanisms of *MITF* induction by UV. Pigment Cell Melanoma Res 23:741–745

Lyons LA, Imes DL, Rah HC, Grahn RA (2005) Tyrosinase mutations associated with Siamese and Burmese patterns in the domestic cat (*Felis catus*). Anim Genet 36:119–126

Manga P, Kromberg JGR, Box NF, Sturm RA, Jenkins T, Ramsay M (1997) Rufous oculocutaneous albinism in Southern African Blacks is caused by mutations in the *TYRP1* gene. Am J Hum Genet 61:1095–1101

Ma L, Parkhurst A, Jeffery WR (2014) The role of a lens survival pathway including *sox2* and *aA-crystallin* in the evolution of cavefish eye degeneration. EvoDevo 5:28

Ma L, Jeffery WR, Essner JJ, Kowalko JE (2015) Genome editing using TALENs in blind Mexican cavefish, *Astynax mexicanus*. PLoS One 10:e0119370

McCauley DW, Hixon E, Jeffery WR (2004) Evolution of pigment cell regression in the cavefish *Astyanax*: a late step in melanogenesis. Evolut Dev 6:209–218

McGaugh SE, Gross JB, Aken B, Blin M, Borowsky R, Chalopin D, Hinaux H, Jeffery WR, Keene A, Ma L, Minx P, Murphy D, O'Quinn KE, Rétaux S, Rohner N, Searle SMJ, Stahl BA, Tabin C, Volff J, Yoshizawa M, Warren WC (2014) The cavefish genome reveals candidate genes for eye loss. Nat Commun 5:5307

Montgomery JC, Coombs S, Baker CF (2001) The mechanosensory lateral line system of the hypogean form of *Astyanax fasciatus*. The biology of hypogean fishes. Springer Netherlands, Dordrecht, pp 87–96

Mortazavi A, Williams BA, McCue K, Schaeffer L, Wold B (2008) Mapping and quantifying mammalian transcriptomes by RNA-seq. Nat Methods 5:621–628

Müller G, Ruppert S, Schmid E, Schütz G (1988) Functional analysis of alternatively spliced tyrosinase gene transcripts. EMBO J 7:2723

O'Quin KE, Yoshizawa M, Doshi P, Jeffery WR (2013) Quantitative genetic analysis of retinal degeneration in the blind cavefish *Astyanax mexicanus*. PLoS ONE 8:e57281-11

Oetting WS (2000) The tyrosinase gene and oculocutaneous albinism type 1 (*OCA1*): a model for understanding the molecular biology of melanin formation. Pigment Cell Res 13:320–325

Oetting WS, Brilliant MH, King RA (1996) The clinical spectrum of albinism in humans. Mol Med Today 2:330–335

Protas ME, Conrad M, Gross JB, Tabin C, Borowsky R (2007) Regressive evolution in the Mexican cave tetra, *Astyanax mexicanus*. Curr Biol 17:452–454

Protas ME, Patel NH (2008) Evolution of coloration patterns. Annu Rev Cell Dev Biol 24:425–446

Protas ME, Hersey C, Kochanek D, Zhou Y, Wilkens H, Jeffery WR, Zon LI, Borowsky R, Tabin CJ (2005) Genetic analysis of cavefish reveals molecular convergence in the evolution of albinism. Nat Genet 38:107–111

Raposo G, Marks MS (2002) The dark side of lysosome-related organelles: Specialization of the endocytic pathway for melanosome biogenesis. Traffic 3:237–248

Raposo G, Tenza D, Murphy DM, Berson JF, Marks MS (2001) Distinct protein sorting and localization to premelanosomes, melanosomes, and lysosomes in pigmented melanocytic cells. J Cell Biol 152:809–824

Rees JL (2003) Genetics of hair and skin color. Annu Rev Genet 37:67–90

Rooryck C, Roudaut C, Robine E, Müsebeck J, Arveiler B (2006) Oculocutaneous albinism with *TYRP1* gene mutations in a Caucasian patient. Pigment Cell Res 19:239–242

Schmidt-Küntzel A, Eizirik E, O'Brien SJ, Menotti-Raymond M (2005) *Tyrosinase* and *Tyrosinase Related Protein 1* alleles specify domestic cat coat color phenotypes of the *albino* and *brown* loci. J Hered 96:289–301

Schmutz SM, Berryere TG (2007) Genes affecting coat colour and pattern in domestic dogs: a review. Anim Genet 38:539–549

Schmutz SM, Dreger DL (2013) Interaction of *MC1R* and *PMEL* alleles on solid coat colors in Highland cattle. Anim Genet 44:9–13

Schonthaler HB, Lampert JM, von Lintig J, Schwarz H, Geisler R, Neuhauss SC (2005) A mutation in the *silver* gene leads to defects in melanosome biogenesis and alterations in the visual system in the zebrafish mutant *fading vision*. Dev Biol 284:421–436

Solano F, Martínez Esparza M, Jimenez-Cervantes C, Hill SP, Lozano JA, García-Borrón JC (2000) New insights on the structure of the mouse *silver* locus and on the function of the *silver* protein. Pigment Cell Res 13:118–124

Spanakis E, Lamina P, Bennett DC (1992) Effects of the developmental colour mutations silver and recessive spotting on proliferation of diploid and immortal mouse melanocytes in culture. Development 114:675–680

Stahl BA, Gross JB (2017) A comparative transcriptomic analysis of development in two *Astyanax* cavefish populations. J ExpZool Part B: Mol Dev Evolut 328:515–532

Sulem P, Gudbjartsson DF, Stacey SN, Helgason A, Rafnar T, Jakobsdottir M, Steinberg S, Gudjonsson SA, Palsson A, Thorleifsson G, Pálsson S, Sigurgeirsson B, Thorisdottir K, Ragnarsson R, Benediktsdottir KR, Aben KK, Vermeulen SH, Goldstein AM, Tucker MA, Kiemeney LA, Olafsson JH, Gulcher J, Kong A, Thorsteinsdottir U, Stefansson K (2008) Two newly identified genetic determinants of pigmentation in Europeans. Nat Genet 40:835–837

Theos AC, Truschel ST, Raposo G, Marks MS (2005) The *Silver* locus product *Pmel17/gp100/Silv/ME20*: controversial in name and in function. Pigment Cell Res 18:322–336

Theos AC, Watt B, Harper DC, Janczura KJ, Theos SC, Herman KE, Marks MS (2013) The PKD domain distinguishes the trafficking and amyloidogenic properties of the pigment cell protein *PMEL* and its homologue *GPNMB*. Pigment Cell Melanoma Res 26:470–486

Valverde P, Healy E, Jackson I, Rees JL, Thody AJ (1995) Variants of the *melanocyte-stimulating hormone receptor* gene are associated with red hair and fair skin in humans. Nat Genet 11:328–330

Wingert RA, Brownlie A, Galloway JL, Dooley K, Fraenkel P, Axe JL, Davidson AJ, Barut B, Noriega L, Sheng X, Zhou Y, Zon LI (2004) The chianti zebrafish mutant provides a model for erythroid-specific disruption of *transferrin receptor 1*. Development 131:6225–6235

Xu S, Hu Z (2010) Mapping quantitative trait loci using distorted markers. Int J Plant Genomics 2009:1–11

Zhang MQ, Xu X, Luo SJ (2014) The genetics of brown coat color and white spotting in domestic yaks (*Bos grunniens*). Anim Genet 45:652–659